Discrimination of Various Poly(propylene) Copolymers and Prediction of Their Ethylene Content by Near-Infrared and Raman Spectroscopy in Combination with Chemometric Methods

Tsuyoshi Furukawa,[1,†] Masahiro Watari,[2] Heinz W. Siesler,[3] Yukihiro Ozaki[1,‡]

[1]*Department of Chemistry, School of Science, Kwansei Gakuin University, Nishinomiya 662-8501, Japan*
[2]*Industrial Measurement Division, Yokogawa Electric Company, Musashino, Tokyo 180-8750, Japan*
[3]*Department of Physical Chemistry, University of Essen, Essen D-45117, Germany*

Received 11 May 2001; accepted 12 April 2002

ABSTRACT: Near-infrared (NIR) diffuse reflectance (DR) spectra and Fourier-transform (FT) Raman spectra were measured for 12 kinds of block and random poly(propylene) (PP) copolymers with different ethylene content in pellets and powder states to propose calibration models that predict the ethylene content in PP and to deepen the understanding of the NIR and Raman spectra of PP. Band assignments were proposed based calculation of the second derivatives of the original spectra, analysis of loadings and regression coefficient plots of principal component analysis (PCA) and principal component regression (PCR) (predicting the ethylene content) models, and comparison of the NIR and Raman spectra of PP with those of linear low-density polyethylene (LLDPE) with short branches. PCR and partial least squares (PLS) regression were applied to the second derivatives of the NIR spectra and the NIR spectra after multiplicative scatter correction (MSC) to develop the calibration models. After MSC treatment, the original spectra yield slightly better results for the standard error of prediction (SEP) than the second derivatives. A plot of regression coefficients for the PCR model shows peaks due to the CH_2 groups pointing upwards and those arising from the CH_3 groups pointing downwards, clearly separating the bands due to CH_3 and CH_2 groups. For the Raman data, MSC and normalization were applied to the original spectra, and then PCR and PLS regression were carried out to build the models. The PLS regression for the normalized spectra yields the best results for the correlation coefficient and the SEP. Raman bands at 1438, 1296, and 1164 cm^{-1} play key roles in the prediction of the ethylene content in PP. The NIR chemometric evaluation of the data gave better results than those derived from the Raman spectra and chemometric analysis. Possible reasons for this observation are discussed. © 2002 Wiley Periodicals, Inc. J Appl Polym Sci 87: 616–625, 2003

Key words: near infrared spectroscopy; diffuse reflectance spectroscopy; Raman spectroscopy; copolymer; poly(propylene) (PP); polyethylene (PE)

INTRODUCTION

Near-infrared (NIR) spectroscopy has frequently been used for polymer analysis for more than two decades.[1–10] However, this field has made remarkable progress within the last five years or so because of advances in NIR spectrometers, detectors, optical light fibers, software, and spectral analysis methods. For example, the development of a variety of NIR instruments has made NIR spectroscopic measurements of polymers much easier and more precise than before. On-line monitoring of molten polymers by NIR light fiber spectroscopy has also become possible.[11–14] Another important reason for the recent progress of NIR spectroscopy of polymers is the advancement in spectral analysis methods. Of particular note are the introduction of two-dimensional (2D) correlation spectroscopy[15–18] to the NIR region and the use of self-modeling curve resolution analysis.[19–21] Thus, the potential of NIR spectroscopy for basic and applied polymer science has been growing steadily over the last several years.

Raman spectroscopy of polymers has a longer history than NIR spectroscopy of polymers.[1,22–27] In the last three decades, Raman spectroscopy has been employed mainly for structural studies of polymers. Band assignments and the Raman spectra–structure relationship have been studied in considerable detail for representative polymers. However, only recently has Raman spectroscopy been used frequently for quantitative and qualitative analysis of polymers, although there were some pioneering studies.[22–27] It was rather difficult to use Raman spectral data for analytical problems because the signal-to-noise ratio

Correspondence to: Y. Ozaki (ozaki@kwansei.ao.jp).
[†]*Present address:* ST Japan Inc., 1-16-27, Minami-Nakaburi, Hirakata 573-0094, Japan
[‡]*Present address:* Department of Chemistry, School of Science, Kwansei Gakuin University, 2-1 Gakuen, Sanda 669-1337

Journal of Applied Polymer Science, Vol. 87, 616–625 (2003)

TABLE I
Ethylene Content of the Investigated Polypropylene (PP) Copolymers

Sample no.	Ethylene content (w/w%)	Classification	
1	6.8	block PP	pellet
2	9.4	block PP	pellet
3	21.5	block PP	pellet
4	10.1	block PP	pellet
5	4.2	random PP	pellet
6	2.8	random PP	pellet
7	2.3	random PP	pellet
8	4.9	random PP	pellet
9	19.7	block PP	pellet
10	9.4	block PP	powder
11	12.8	block PP	powder
12	18.7	block PP	powder

of Raman spectra was not always high and the background of Raman spectra often changed significantly from one spectrum to another. Recent progress in Raman instrumentation has removed those obstacles for analytical applications of Raman spectroscopy.

Until recently, NIR and Raman spectroscopy have rarely been used for the same purpose. The situation has changed dramatically within the last several years, and NIR and Raman spectroscopy often have common applications now.

We have been involved in a series of systematic studies of NIR and Raman spectra of basic polymers.[28–32] Our studies have three major purposes. One purpose is to deepen the understanding and interpretation of NIR and Raman spectra of polymers. Another purpose is to develop nondestructive analytical methods for on-line monitoring of polymers based on NIR and Raman spectroscopy. Yet another purpose is to explore the potential of NIR spectroscopy for the investigation of the structure and conformation of polymers. For these purposes we frequently use conservative spectral analysis methods, such as derivatives, chemometrics, and generalized two-dimensional (2D) correlation spectroscopy, as the need arises.

This particular study aims at proposing calibration models that predict the ethylene content in PP pellets and powders and to analyze the models based on the interpretation of their loadings and regression coefficient plots. Another purpose of the present study is to investigate if one can differentiate between pellet and powder samples and between block and random PP copolymers in a nondestructive manner by NIR and Raman spectroscopy. This study also intends to compare the potential of NIR and Raman spectroscopy for the quantitative and qualitative analysis of polymers. Such a comparison is of importance partly because it allows one to correlate spectral variations observed in the NIR region with those in the fundamental vibration region and partly because one can discuss advantages and disadvantages of NIR and Raman spectroscopy as nondestructive tools for polymer analysis.

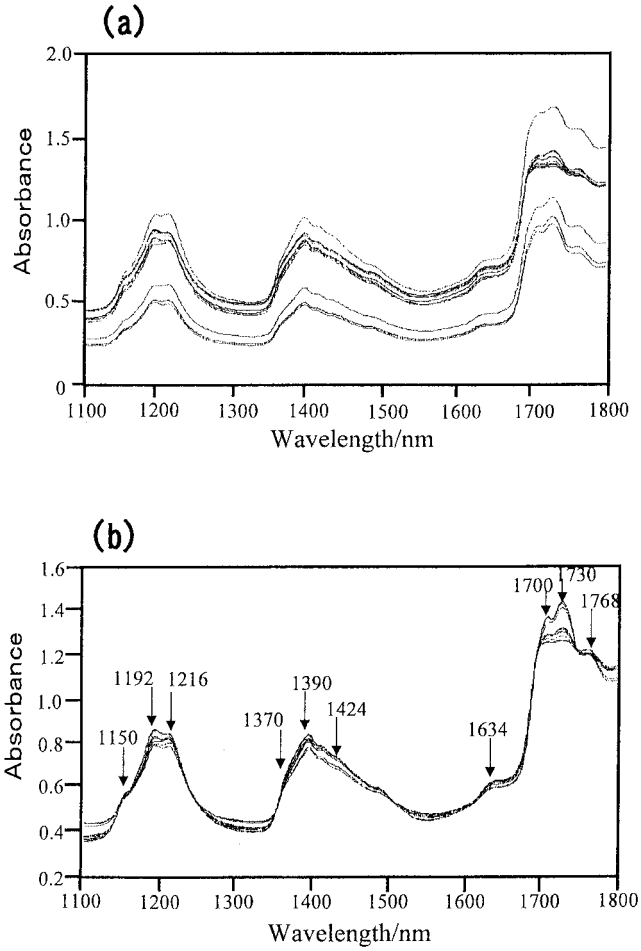

Figure 1 NIR spectra of the investigated PP copolymers (a) before and (b) after MSC treatment.

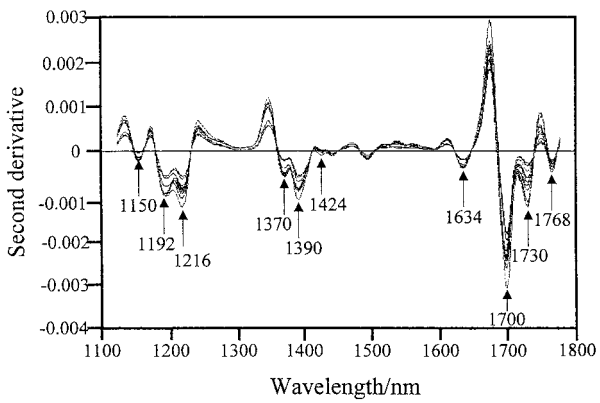

Figure 2 Second derivatives of the NIR spectra shown in Figure 1a.

TABLE II
Assignments of the NIR Bands of PP Copolymers

Wavelength, nm	Assignment
1150	C—H str second overtone (CH_3)
1192	C—H str second overtone (CH_3)
1216	C—H str second overtone (CH_2)
1370	2 × C—H str + C—H def (CH_3)
1390	2 × C—H str + C—H def (CH_2)
1424	2 × C—H str + C—H def (CH_2)
1490	combination (CH_3)
1540	combination (CH_2)
1634	combination (CH_3)
1700	C—H str first overtone (CH_3)
1730	C—H str first overtone (CH_2)
1768	C—H str first overtone (CH_2)

MATERIALS AND METHODS

Samples

Twelve kinds of commercial PP samples with different ethylene concentration (2.3–21.5 wt %) were used without further purification (Table I). Nine samples were obtained as pellets and three samples were received as powders. Five kinds of the pellet samples were PP block copolymers and the rest of the pellet samples were random PP copolymers. All the powder samples were PP block copolymers.

Spectral measurements

The NIR diffuse reflectance (DR) spectra were measured for the 12 kinds of polymer samples with a Bran + Luebbe Infralyser 500 spectrometer at a spectral resolution of 2 nm. The samples were placed on a rotating cup in a drawer to observe the DR radiation uniformly from different portions of the samples.

The Raman spectra were measured for the polymer samples at a spectral resolution of 8 cm^{-1} with a JEOL JIR 6500 FT-Raman spectrometer equipped with an InGaAs detector. The 1064-nm line from a Nd:YAG laser (Spectron) was employed as an excitation line. To ensure a good signal-to-noise ratio, 400 scans were coadded.

Data analysis

The NIR and Raman spectra were measured as repacks five times for each sample. Unscrambler® (version 6.1) software program (CAMO AS, Trondheim, Norway) was employed for spectral data analysis. The NIR spectra in the 1100–1800-nm region were subjected to the multivariate data analyses specified later, and the number of data points for each NIR spectrum was 350. The NIR data were subjected to the treatment of multiplicative scatter correction (MSC) or the sec-

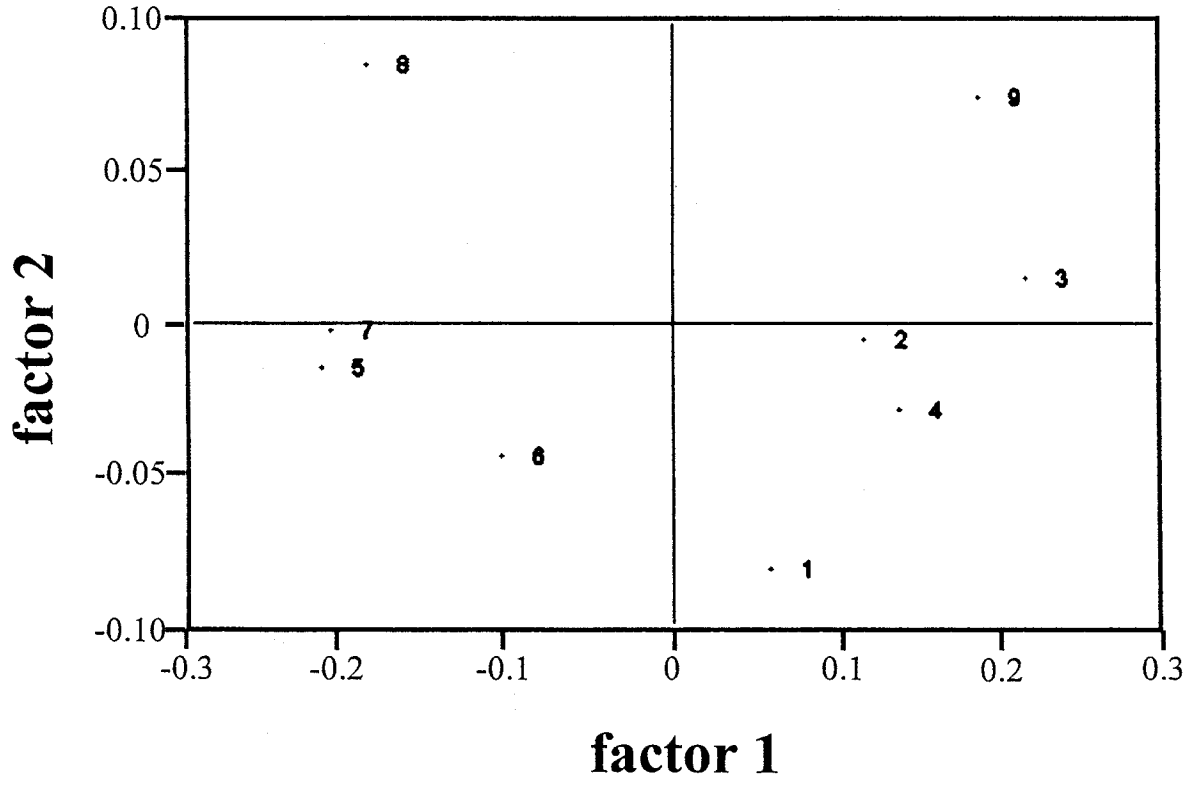

Figure 3 Score plot of PCA factor 1 versus factor 2 for nine different PP copolymers based on their NIR spectra in the 1100–1800-nm region (the NIR spectral data were pretreated by MSC). Numbers adjacent to each point indicate the sample number.

ond—derivative transformation before proceeding with any analyses. Principal component analysis (PCA) was applied to both the NIR and Raman spectral data to discriminate between the pellet and powder samples and between block and random PP copolymers. Principal component regression (PCR) and partial least squares (PLS) regression were applied to develop calibration methods that predict the concentration of ethylene in PP. To produce the calibration models, leave-one-out cross-validation was used.

RESULTS AND DISCUSSION

Band assignments of the NIR spectra of the PP copolymers

The NIR spectra of the PP samples before and after the MSC treatment are shown in Figures 1a and 1b, respectively. The spectra are subdivided into two groups by large spectral changes in the 1650–1800 nm region. Thus, it may be concluded that the NIR pellet and powder samples can be differentiated even by the original spectra.

The second derivatives of the NIR spectra shown in Figure 1a are shown in Figure 2. The second-derivative spectra demonstrate the existence of weak bands at 1150, 1370, and 1424 nm. The band assignments for the NIR spectra of the PP copolymers are summarized in Table II. The assignments are based on the comparison of the spectra of PP with those of polyethylene (PE) with various branches.[28] The band assignments will be discussed later.

PCA of the NIR spectra of the different pellet samples

A score plot of the PCA factors 1 versus 2 for the nine PP pellet samples based on their NIR spectra in the 1100–1800-nm region is illustrated in Figure 3. The NIR spectra of these PP samples were pretreated by MSC. Of note in Figure 3 is that the PP block copolymers have positive score values, whereas the random PP copolymers yield negative score values in factor 1. One could equally well interpret the separation along factor 1 with the ethylene content; Sample 3 has the highest ethylene content. Probably both the ethylene content and block/random copolymers are separated along factor 1.

The PC loadings plots of factor 1 and factor 2 corresponding to the score plot of Figure 3 are presented in Figures 4a and 4b, respectively. The loadings plot for factor 1 shows a negative peak at 1190 nm due to a second overtone of the CH_3 stretching mode and a positive peak at 1730 nm due to a first overtone of the CH_2 stretching mode. However, it should be noted that the loadings plot is very similar to the spectrum of PP up to 1700 nm, although the direction of the peaks is reversed. Therefore, it seems that in spite of the data pretreatment, factor 1 reflects baseline variations. The PP block copolymers have a higher crystallinity than the random PP copolymers, so the former looks white, giving stronger light scattering. We infer that even the MSC treatment cannot completely remove the effect of the baseline variations because of this light scattering effect.

The loadings plot for factor 2 shows positive peaks at 1222 and 1766 nm due to second and first overtones of the CH_2 stretching mode, respectively, and yields negative peaks at 1360, 1490, and 1630 nm assigned to combinations of the CH_3 vibrations. Therefore, the loadings plot for factor 2 separates bands due to the CH_3 and CH_2 groups. This tendency is clearer for the PP block copolymers. In the block copolymers, ethylene blocks and propylene blocks are separated so that each species keeps its own characteristic features.

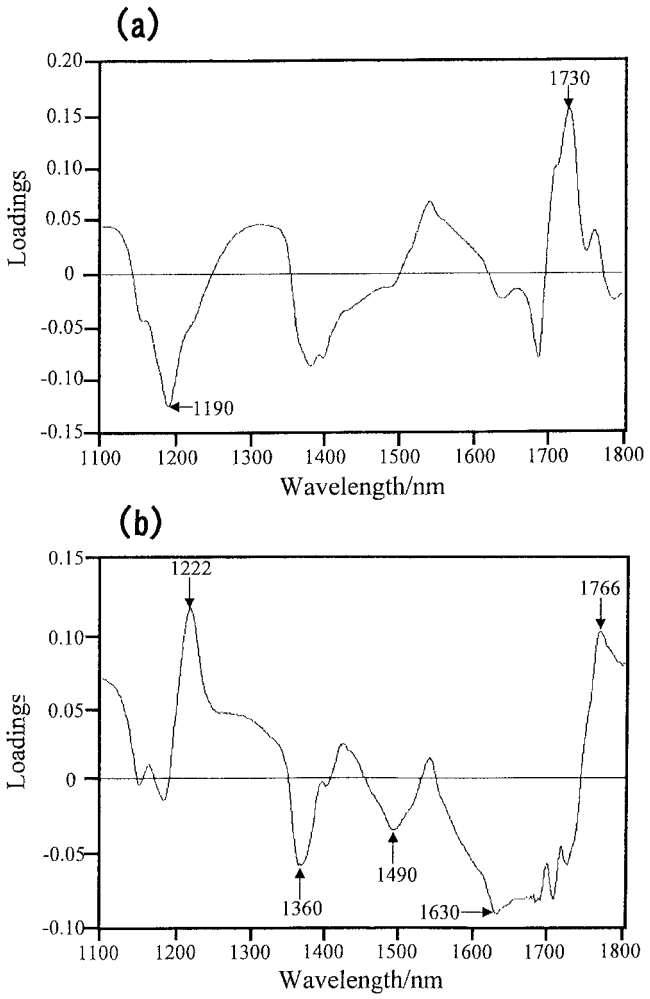

Figure 4 Loadings plots of (a) factor 1 and (b) factor 2 for the PCA model represented by the score plot of Figure 3.

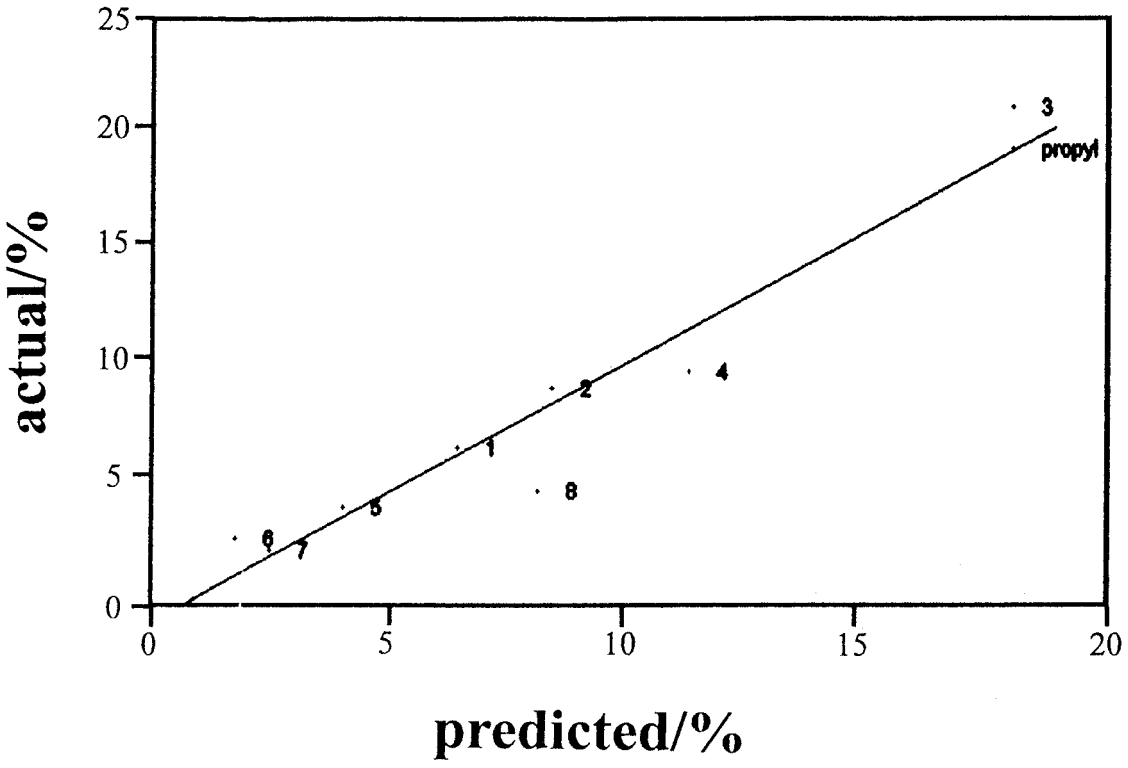

Figure 5 A PCR regression calibration model for the prediction of the ethylene content in PP copolymers from the NIR spectra after the MSC treatment.

Prediction of the concentration of ethylene in PP by PCR and PLS regression

The PCR regression calibration model for predicting the ethylene content in the PP copolymers from the NIR spectra after the MSC treatment is shown in Figure 5. A plot of the residual variance of the PCR regression showed that two factors were enough for the prediction. A good straight line could be obtained between the actual and predicted values. We tried to calculate PCR and PLS regression calibration models for the spectra after the MSC treatment and after second-derivative transformation. The correlation coefficients (R) and standard errors of prediction (SEP) for all the trials are summarized in Table III. The MSC treatment yields better results than the second-derivative transformation. In the prediction of physical properties of polymers by NIR spectroscopy, MSC generally gives better results than other pretreatments.[28,29]

A plot of Lee and Chung[33] also reported the prediction of the ethylene content by NIR spectroscopy, although they did not discuss plots of the regression coefficients (RC) for the models. They used the second-derivative spectra for developing the models. RC for the PCR model shown in Figure 5 is depicted in Figure 6. Positive peaks appear at 1220, 1420, 1540, 1730, and 1764 nm, whereas negative peaks appear at 1150, 1190, 1370, 1492, and 1700 nm. All the positive

TABLE III
Correlation Coefficient (R) and Standard Error of Prediction (SEP) for Various Calibration Models Developed from the NIR Data

Multivariate analyses	Pretreatment	R	SEP (%)
PCR	2nd derivative	0.98	1.71
	MSC	0.99	0.80
PLS regression	2nd derivative	0.99	1.32
	MSC	0.99	0.94

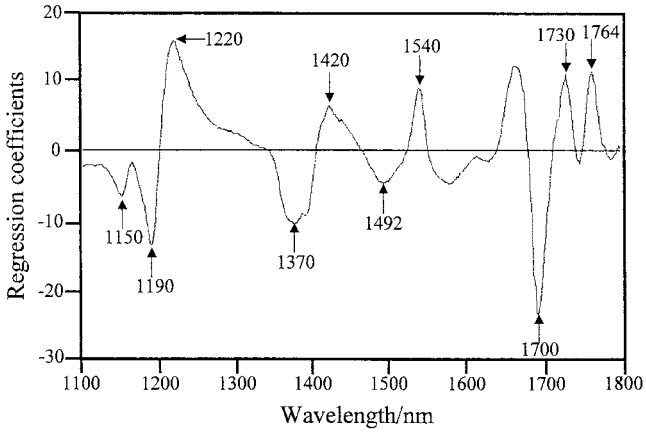

Figure 6 A plot of regression coefficients for the PCR calibration model shown in Figure 5.

TABLE IV
Assignments of the NIR Bands of LLDPE

Band, nm	Assignment
1146	C—H str second overtone (CH_3)
1166	C—H str second overtone (CH_2)
1186	C—H str second overtone (CH_3)
1214	C—H str second overtone (CH_2)
1300	(CH_2)
1374	2 C—H str + C—H def (CH_3)
1392	2 C—H str + C—H def (CH_2)
1416	2 C—H str + C—H def (CH_2)
1542	(CH_2)
1634	(CH_3)
1698	C—H str first overtone (CH_3)
1710	(CH_2)
1728	C—H str first overtone (CH_2)
1764	C—H str first overtone (CH_2)

peaks are attributed to the CH_2 groups and all the negative peaks are assigned to the CH_3 groups. Therefore, the bands arising from the CH_3 and CH_2 groups appear in the RC plot with opposite signs. The separation between the CH_3 and CH_2 bands is clearer in the RC plot for the PCR model (Figure 6) than in the loadings plot for the PCA model (Figure 4b) because in the PCR model, the y-values (PE concentrations) are taken into account, whereas the PCA model is only based on spectral features.

Comparison of NIR spectra of PP with those of LLDPE

It is of particular interest to compare NIR spectra of PP with those of linear low density polyethylene (LLDPE) samples from two major points of view. One is that the comparison between the NIR spectra of PP and LLDPE is very useful to establish the band assignments

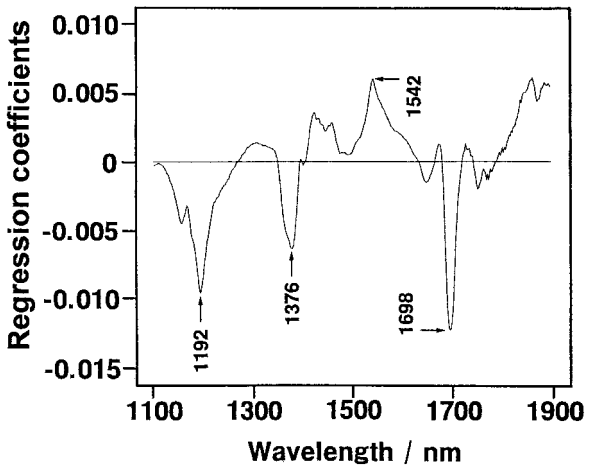

Figure 7 A plot of regression coefficient for a PCR model predicting the density of LLDPE from NIR spectra after MSC treatment (reproduced from ref [28] with permission; copyright 1998, NIR Publications).

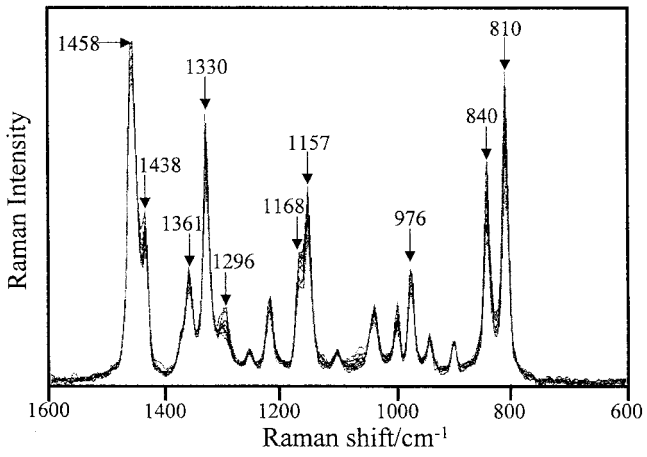

Figure 8 FT-Raman spectra of the investigated PP copolymers after MSC treatment.

for the NIR spectra of these basic polymers. The NIR spectra of both PP, and LLDPE consist solely of bands due to the CH_3 and CH_2 groups, but apparently the spectra of PP show bands due to the CH_3 groups more strongly. Therefore, the comparison may allow one to distinguish the CH_3 bands from the CH_2 bands. Another important point in the comparison is that for both PP and LLDPE, RC plots for models predicting their physical properties separate bands due to the CH_3 and CH_2 groups, and thus the comparison of these plots may make their interpretation easier. In both PP and LLDPE, the ratio of the populations of the CH_2 and CH_3 groups is concerned with their physical properties, such as density and crystallinity. Therefore, the comparison between the NIR spectra of PP and LLDPE is useful to establish a relation between the NIR spectra and the physical properties.

The previously reported band assignments for an NIR spectrum of LLDPE are shown in Table IV.[28] Comparison of Tables II and IV reveals that the band assignments for PP and LLDPE are in good agreement with each other. The frequencies of the CH_3 and CH_2 bands of PP are fairly close to those of LLDPE.

A plot of regression coefficients for a PCR model predicting the density of LLDPE from NIR spectra

TABLE V
Assignment of Raman Bands of PP Copolymers

Raman shift, cm^{-1}	Assignment
1458	CH_2 scissoring
1438	CH_2 scissoring
1361	CH_3 symmetric deformation
1330	CH_2 twisting
1296	CH_2 twisting
1168	C—C stretching
1157	C—C stretching
976	CH_3 rocking
840	CH_3 rocking
810	C—C stretching

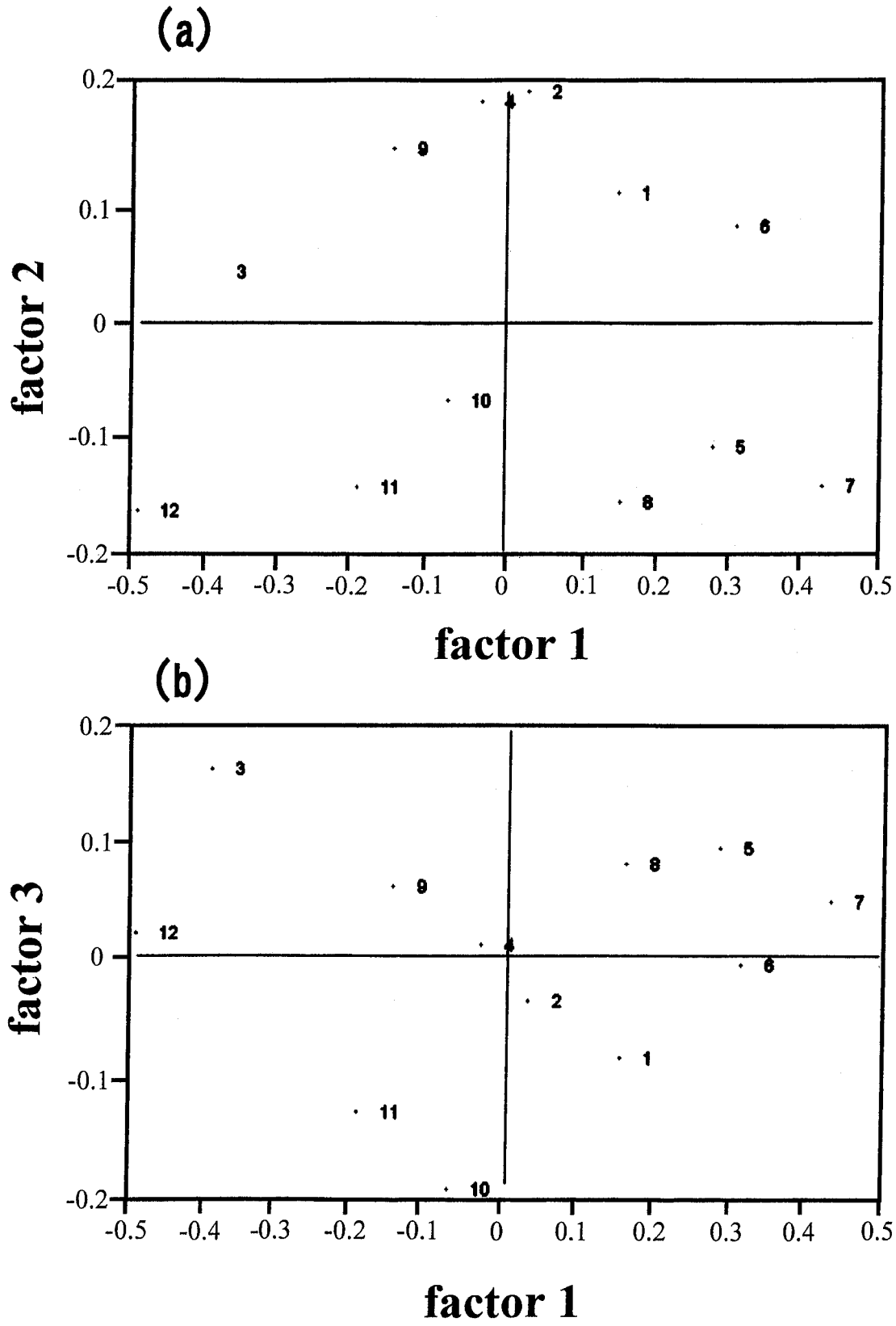

Figure 9 Score plot of (a) PCA factor 1 versus factor 2 and (b) PCA factor 1 versus factor 3 for the 12 PP copolymers based on their Raman spectra in the 1600–600-cm^{-1} region. The Raman spectra were pretreated by MSC, and the numbers adjacent to each point indicate the sample number.

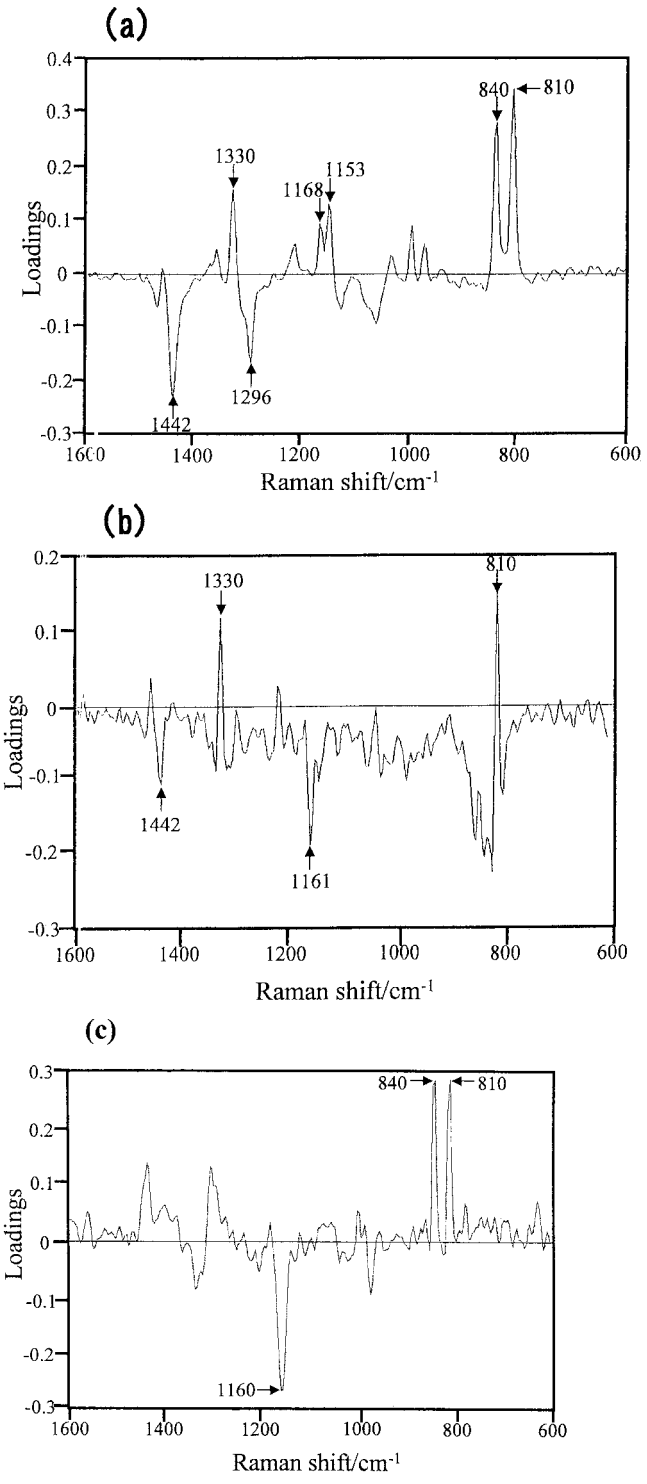

Figure 10 Loadings plots of (a) factor 1, (b) factor 2, and (c) factor 3 for the PCA model of the score plots shown in Figure 8.

after MSC treatment is shown in Figure 7.[28] It is noted that the RC plots of PP (Figure 6) and LLDPE (Figure 7) are similar to each other, but the former shows the upward peaks due to the CH_2 groups more clearly.

BAND ASSIGNMENTS FOR THE RAMAN SPECTRA OF PP

The FT-Raman spectra of the 12 PP copolymer samples after the MSC treatment are shown in Figure 8. Raman spectra of PP have been investigated in considerable detail, thus the band assignments are straightforward for the major bands.[1,34–36] The band assignments for the Raman spectra of PP are summarized in Table V. It can be seen in Figure 8 that significant intensity changes appear at 1438, 1296, and 1168 cm^{-1}, which are all due to the CH_2 groups.

Score plots of PCA factor 1 versus factor 2 and of factor 1 versus factor 3 for the 12 PP samples based on their Raman spectra in the 1600–600-cm^{-1} region are shown in Figures 9a and 9b, respectively. The samples with the higher ethylene concentration give smaller score values in factor 1. As for factor 2, PP block copolymer in pellets yield positive score values, whereas PP block copolymers in powders and random PP yield negative score values. In both Figures 9a and 9b, the 12 PP copolymers are classified into three groups; they are, PP block copolymers in pellets, PP blockcopolymers in powders, and random PP copolymers.

The PC loadings plots of factor 1, factor 2, and factor 3 are depicted in Figures 10a, 10b, and 10c, respectively, for the score plots shown in Figure 9. The loadings plot for factor 1 shows positive bands at 1330, 1168, 1153, 840, and 810 cm^{-1} and negative bands at 1442 and 1296 cm^{-1}. All the positive bands arise from CH_3 groups or C—C bonds, whereas all the negative bands are due to CH_2 groups. Thus, the loadings plot of factor 1 is concerned with the concentration of ethylene and separates bands into two groups, the bands due to CH_3 and C—C functionalities and those assigned to CH_2 groups.

Prediction of the ethylene content in PP copolymers by PLS regression

A PLS regression calibration model for predicting ethylene content in PP copolymers from the Raman spectra after MSC treatment is shown in Figure 11a. A plot of the residual variance of the PLS regression showed that three factors provided a satisfactory prediction. We developed four models with PCR and PLS regression for the Raman spectra of the 12 PP copolymers samples after MSC or normalization. The values of *R* and SEP for these four models are compared in Table VI. It can be seen from the results in Table VI that the PLS regression for the Raman spectra after normalization yields slightly better results than the other calibration models.

A plot of regression coefficients for the PLS calibration model shown in Figure 11a is depicted in Figure 11b. This RC plot is similar to the loadings plot for

PCA factor 1 (Figure 10a). Two upward peaks appear at 1438 and 1296 cm^{-1} and two downward peaks appear at 1164 and 810 cm^{-1}.

Again, the bands due to the CH_2 groups and those arising from the CH_3 groups and C—C bonds are separated in the plot. It is noted that the intensity changes at 1438, 1296, and 1164 cm^{-1} are prominent even in the original spectra (Figure 7).

Comparison between NIR and Raman spectroscopy

Comparison of Table III and Table VI reveals that NIR spectroscopy yields much better results than Raman spectroscopy for the investigated PP copolymers. The number of samples is too small to make fair comparison between NIR and Raman spectroscopy as a nondestructive analytical probe for the polymers. The possible reason for the significant differences in the correlation coefficient and SEP between NIR and Raman spectroscopy is that NIR DR spectroscopy measures the spectra of whole polymer samples, whereas Raman spectroscopy probes only a small volume of the polymer samples under investigation. Another possible reason is that most of the bands appearing in the NIR spectra of PP copolymers are due to the CH_3 and CH_2 groups, whereas they are due to the different excitation conditions in the Raman spectra bands because C—C stretching modes are strongly accentuated. Thus, the ethylene group may be more clearly differentiated in the NIR spectra. However, in the case of PE pellet samples, NIR and Raman spectroscopy give very similar results for the prediction of the density.[36] Thus, probably, the two spectroscopic techniques accentuate different features in the different polymers. Further studies are needed for the comparison of the potential of nondestructive analysis tools between NIR and Raman spectroscopy.

TABLE VI
Correlation Coefficient (*R*) and Standard Error of Prediction (SEP) for Various Calibration Models

Multivariate analyses	Pretreatment	*R*	SEP (%)
PCR	Normalization	0.92	2.59
	MSC	0.94	2.27
PLS regression	Normalization	0.95	2.15
	MSC	0.94	2.30

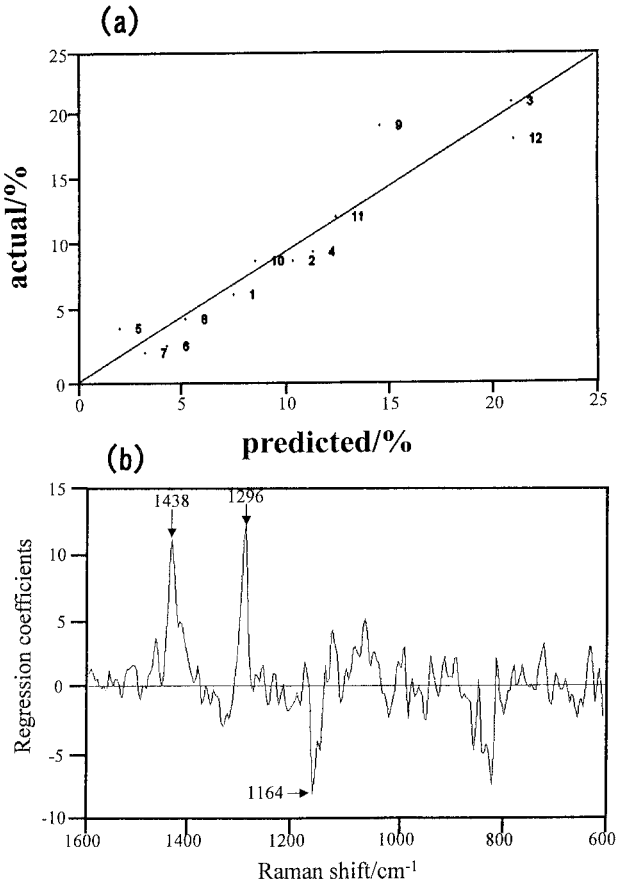

Figure 11 (a) A PLS regression calibration model for predicting the ethylene content in PP copolymers from the Raman spectra after MSC treatment. (b) A plot of regression coefficients for the PLS calibration model shown in (a).

CONCLUSIONS

In this paper, we have demonstrated the potential of NIR and Raman spectroscopy in combination with multivariate data analysis for the prediction of the ethylene content in PP copolymers. The NIR spectra of nine kinds of PP copolymers (five block copolymers and four random copolymers) were subjected to a PCA analysis and a PCR regression, and the loadings and regression coefficient plots were used to support the NIR spectroscopic assignments. Different calibration models for the prediction of the ethylene content in the PP copolymers were developed on the bases of PCR and PLS regression and compared in terms of their performance.

References

1. Siesler, H. W.; Holland-Moritz, K. Infrared and Raman Spectroscopy of Polymers, Practical Spectroscopy Series Vol. 4, Marcel Dekker: New York, 1980.
2. Miller, C. E. Appl Spectrosc Rev 1991, 26, 277.
3. Siesler, H. W. Macromol Chem Macromol Symp 1991, 5, 113.
4. Handbook of Near-Infrared Analysis; Burns, D. A.; Ciurczak, E. W. Eds., Marcel Dekker: New York, 1992.
5. Lee, K. A. B. Appl Spectrosc Rev 1993, 28, 231.
6. Molt, K., Ihlbrock, D. Fresenius J Anal Chem 1994, 348, 523.
7. Chabert, B.; Lachenal, G.; Vinh Tung, C. Macromol Chem Macromol Symp 1995, 94, 145.
8. Lachenal, G. Vib Spectrosc 1995, 9, 93.
9. van Uum, M. P. B.; Lammers, H.; de Kleijin, J. P. Macromol Chem Phys 1995, 196, 2023.
10. Dumoulin, M. M.; Gendron, R.; Cole, K. C. TRIP 1996, 4, 109.

11. Ozaki, Y.; Amari, T. In Spectroscopy in Process Analysis; Chalmers, J. M., Ed., Sheffield Academic Press: Sheffield, U.K., 2000; p. 53.
12. Ḳhettry, A.; Hansen, M. G. Polym Eng Sci 1996, 36, 1232.
13. Šašic, S.; Kita, Y.; Furukawa, T.; Watari, M.; Siesler, H. W.; Ozaki, Y. Analyst 2000, 125, 2315.
14. Bandermann, F.; Tausendfreund, I.; Šašic, S.; Ozaki, Y.; Kleimann, M.; Westerhuis, J. A.; Siesler, H. W. Macromol Rapid Commun, in press.
15. Noda, I. Appl Spectrosc 1993, 47, 1329.
16. Noda, I.; Dowrey, A. E.; Marcott, C.; Story, G. M.; Ozaki, Y. Appl Spectrosc 2000, 54, 236A.
17. Noda, I. Appl Spectrosc 2000, 54, 994.
18. Two-Dimensional Correlation Spectroscopy, Ozaki, Y.; Noda, I., Eds.; American Institute of Physics: New York, 2000.
19. Vandeginste, B. G. M.; Massart, D. L.; Buydens, L. M. C.; de Jong, S.; Lewi, P. J.; Smeyers-Verbecke, J. Handbook of Chemometrics and Qualimetrics; Elsevier: Amsterdam, 1998.
20. Tauler, R.; Kowalski, B. R.; Fleming, S. Anal Chem 1998, 65, 2040.
21. Gemperline, P. J. Anal Chem 1998, 69, 5318.
22. Polymer Spectroscopy; Hummel, D. O., Ed.; Verlag Chemie: Weinheim, 1974.
23. Klöpffer, W. Introduction to Polymer Spectroscopy; Springer-Verlag: New York, 1984; Chapter 6.
24. Batchelder, D. N.; Chang, C.; Pitt, G. D. Adv Mater 1991, 3, 566.
25. Polymer Spectroscopy; Fawcett, A. H., Ed.; John Wiley & Sons: Chichester, U. K., 1996, Chapters 7 and 8.
26. Everall, N.; Tayler, P.; Chalmers, J.; Ferweerda, R.; van der Maas, J. Polymer, 1994, 35, 3184.
27. Zerbi, G.; Del Zoppo, M. In Modern Polymer Spectroscopy; G. Zerbi G., Ed.; Wiley-VCH: Weinheim, 1999; p. 87.
28. Shimoyama, M.; Sano, K.; Higashiyama, H.; Watari, M.; Tomo, M.; Ninomiya, T.; Ozaki, Y. J Near Infrared Spectrosc 1998, 6, 317.
29. Shimoyama, M.; Hayano, S.; Matsukawa, K.; Inoue, H.; Ninomiya, T.; Ozaki, Y. J Polym Sci, Polym Phys Ed 1998, 36, 1529.
30. Sano, K.; Shimoyama, M.; Ohgane, M.; Higashiyama, H.; Watari, M.; Tomo, M.; Ninomiya, T.; Ozaki, Y. Appl Spectrosc 1999, 53, 551.
31. Ren, Y.; Shimoyama, M.; Ninomiya, T.; Matsukawa, K.; Inoue, H.; Noda, I.; Ozaki, Y. Appl Spectrosc 1999, 53, 919.
32. Ren, Y.; Shimoyama, M.; Ninomiya, T.; Matsukawa, K.; Inoue, H.; Noda, I.; Ozaki, Y. J Phys Chem 1999, 103 B, 6475.
33. Lee, J.-S.; Chung, H. Vib Spectrosc 1998, 17, 193.
34. Masetti, G.; Cabassi, F.; Zerbi, G. Polymer 1980, 21, 143.
35. Zerbi, G. Specialist Reports 1983, 203, 501.
36. Sunsell, T.; Fagerholm, H.; Crozier, H. Ḍolymer 1996, 37, 3227.
37. Sato, H.; Shimoyama, M.; Kamiya, T.; Šašic, S.; Amari, T.; Ninomiya, T.; Siesler, H. W.; Ozaki, Y. submitted.